UDC 621.314 https://doi.org/10.20998/2074-272X.2023.2.08

D. Sakri, H. Laib, S.E. Farhi, N. Golea

Sliding mode approach for control and observation of a three phase AC-DC pulse-width modulation rectifier

Introduction. *For AC-DC conversion systems, the electrical systems typically use thyristor or diode bridge rectifiers, which have relatively poor performance. Nowadays, three-phase pulse-width modulation rectifiers are widely applied in various applications for their well-known intrinsic benefits, such as adjustable DC link voltage, unity power factor, bidirectional power flow and very low total harmonic distortion.* ***Purpose****. The objective of this work is to achieve better stability and dynamic performance using sliding mode strategy for control and observation.* ***Methods****. For that purpose, first a sliding mode controller is introduced on the DC-link side to ensure a fast and accurate response of the output load voltage. Then, the sliding mode approach is employed to control the quadrature and direct components of power to maintain the input power factor at unity. Finally, this approach is used to design two observers for grid voltage estimation and online variation of load resistance. To overcome the problem associated with the use of the classical low-pass filter, an adaptive compensation algorithm is used to compensate the attenuation of the amplitude and phase delay of the observed grid voltages. This algorithm is based on the use of the two low-pass filters in cascade and ensures the minimization of chattering.* ***Results****. Comparative studies have been carried out between sliding mode control method for controlling the three-phase AC-DC pulse-width modulation rectifier and other conventional techniques. The validation by simulation and the tests carried out gave very satisfactory results and proved the effectiveness and feasibility of the sliding mode for both control and observation of three phase pulse-width modulation rectifier.* References 25, table 2, figures 19.

Key words: **direct power control, three phase pulse-width modulation rectifier, sliding mode control, double-low pass filter, unity power factor.**

Вступ*. Для AC-DC систем перетворення електричні системи зазвичай використовують тиристорні або діодні мостові випрямлячі, які мають відносно погані характеристики. В даний час трифазні випрямлячі з широтно-імпульсною модуляцією широко застосовуються з різними цілями завдяки їх добре відомим внутрішнім перевагам, таким як регульована напруга у ланці постійного струму, одиничний коефіцієнт потужності, двонаправлений потік потужності та дуже низькі загальні гармонічні спотворення.* ***Метою*** *даної роботи є досягнення кращої стабільності та динамічних характеристик з використанням стратегії ковзного режиму для контролю та спостереження.* ***Методи****. З цією метою спочатку на стороні ланки постійного струму вводиться регулятор режиму ковзання, щоб забезпечити швидку і точну реакцію на вихідну напругу навантаження. Потім використовується метод ковзного режиму для управління квадратурною та прямою складовими потужності, щоб підтримувати вхідний коефіцієнт потужності рівним одиниці. Нарешті цей підхід використовується для розробки двох спостерігачів для оцінки напруги мережі та зміни опору навантаження в режимі онлайн. Для подолання проблеми, пов'язаної з використанням класичного низькочастотного фільтру, використовується алгоритм адаптивної компенсації, що компенсує загасання амплітуди і фазової затримки напруг мережі, що спостерігаються. Цей алгоритм заснований на використанні двох низькочастотних фільтрів у каскаді та забезпечує мінімізацію брязкоту.* ***Результати****. Були проведені порівняльні дослідження між методом керування ковзним режимом для керування трифазним випрямлячем AC-DC з широтно-імпульсною модуляцією та іншими традиційними методами. Перевірка за допомогою моделювання та проведені випробування дали дуже задовільні результати та довели ефективність та здійсненність ковзного режиму як для управління, так і для спостереження за трифазним випрямлячем з широтно-імпульсною модуляцією.* Бібл. 25, табл. 2, рис. 19.

Ключові слова: **пряме керування потужністю, трифазний випрямляч з широтно-імпульсною модуляцією, ковзне керування, подвійний низькочастотний фільтр, одиничний коефіцієнт потужності.**

Introduction. In recent years, advances in the field of power electronics have contributed to the development of new static converter structures that allow the modulation of electrical energy according to industrial use. These converters are widely used in industrial or domestic fields, such as non-controlled diodes and controlled thyristor rectifiers. These converters behave like non-linear loads, absorbing harmonic currents that have a very negative impact on the electrical grid. Indeed, it can cause a number of disturbances, ranging from equipment dysfunction to complete destruction.

Harmonic pollution is a phenomenon that leads to the degradation of power quality, especially the distortion of the voltage wave, which increases the rate of harmonic distortion of the current that can exceed a value of 30 % [1]. Unfortunately, this value does not conform to the international standards imposed by the specialized organisms: IEC 61000, EN 50160 and IEEE Standard 519 which impose total harmonic distortion (THD) limits of 3 % for voltages and 5 % for currents [1]. In this situation, and to overcome this kind of problem, several solutions have been developed: curative solutions such as active filters and preventive solutions such as pulse width modulation rectifiers. Low harmonic pollution, controllable reactive power, adjustable DC-link voltage, unit power factor and bi-directional power flow are some advantages of this converter topology [2-7].

Because of its higher performances than the traditional thyristor or diode rectifier bridge, the three-phase pulse-width modulation (PWM) rectifier is now widely utilized in industry, including power supplies for microelectronics, wind power production, telecommunications equipment, etc [8]. The design of these non-polluting converters, combined with a judicious choice of control, provides a significant improvement current waveform of the electrical grid and guarantees operation with a unity power factor.

In this context, many techniques have been applied to three-phase PWM rectifiers to improve power quality. Voltage-oriented control, which derives from field-oriented control applied to AC machines, is one of the efficient techniques that permit decoupled control. It consists of eliminating the voltage quadrature component in order to ensure an indirect and decoupled control of the power. The voltage references for the direct and quadrature components are generated from the current controllers in the rotating frame. Since position data is necessary for all d-q transformations in voltage-oriented

control, position information can be obtained via estimation of the virtual flux or from measurement or observation of grid voltages. As for the reference of the direct current component, it is obtained from the regulation of DC-link voltage, while the reference of the quadrature component is set to zero in order to have a unitary power factor operation.

By analogy to the direct torque control of AC machines in the stationary α-β frame, another control technique for PWM rectifiers proposed by Ohnishi in 1991 so-called direct power control (DPC) and later developed by Takahachi and Noguchi in 1998 [9, 10].

In DPC, it is possible to control directly the active and reactive power by selecting the appropriate inverter state from a predefined switching table. For each sampling time, the appropriate inverter voltage vectors are selected according to the errors between the active and reactive powers and their references and the position of the voltage vector. The active power reference is provided by a PI controller for DC-link voltage while the reactive power reference is maintained at zero to ensure unity power factor. Two DPC configurations can be used: DPC based on measured or estimated voltage vectors (V-DPC) [1, 9, 11-12]: the position is determined by voltage vectors, and the instantaneous powers are calculated from voltage and current vectors. DPC based on virtual flux [1, 13-16]: where the estimated fluxes define the position and the instantaneous powers are calculated from the current and fluxes vectors. However, the classical direct power control has many disadvantages, such as: a variable switching frequency due to the hysteresis comparators, a high filter inductance value to obtain a smooth current, a low sampling period is required for accurate power estimation, and its implementation requires a fast microprocessor and an ADC due to its high sampling frequency requirement [17].

In order to improve the classical DPC, this strategy is combined with the sliding mode control (SMC) approach, which is distinguished by its robustness to parametric variations and external perturbations [18, 19]. In addition, the SMC is used to design simple, efficient and more economical observers which eliminates the need for physical sensors and reduces cost.

In this perspective, this paper aims to improve the dynamic and static performances of direct power control using the sliding mode approach. This improvement can be illustrated by comparison with other techniques in terms of THD and power factor. To achieve these objectives, enhancements have been introduced by:

- substituting the PI controller of the DC-link voltage with SMC;
- ensuring direct and decoupled control for both active and reactive power;
- replacing grid voltage sensors with a sliding mode observer combined with a double-low-pass filter to minimize the chattering phenomenon and to compensate amplitude attenuation and phase errors;
- on-line estimating variation in load resistance.

Three phase PWM rectifier model. A three-phase PWM rectifier's topology is given by Fig. 1, where i_a, i_b, i_c and e_a, e_b, e_c are the three-phase grid currents and voltages, V_a, V_b, V_c are the input voltages of three-phase PWM rectifier, L and R are the inductance and resistance of interconnecting filters and R_L is the load resistor of the DC side.

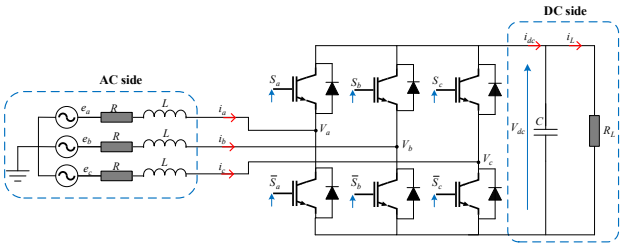

Fig. 1. Electrical circuit of a three phase PWM rectifier

According to the per phase equivalent circuit in Fig. 2, the AC side equations can be given as:

$$\begin{cases} L\dfrac{di_a}{dt} = e_a - Ri_a - V_a; \\ L\dfrac{di_b}{dt} = e_b - Ri_b - V_b; \\ L\dfrac{di_c}{dt} = e_c - Ri_c - V_c. \end{cases} \quad (1)$$

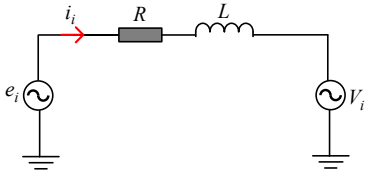

Fig. 2. Per phase model of three phase PWM rectifier

For the DC side, the equation is written as:

$$C\frac{\mathrm{d}V_{dc}}{\mathrm{d}t} = (S_a i_a + S_b i_b + S_c i_c) - \frac{V_{dc}}{R_L}. \quad (2)$$

In the (α, β) frame, the three-phase boost rectifier model can be written as:

$$\begin{cases} L\dfrac{\mathrm{d}i_\alpha}{\mathrm{d}t} = e_\alpha - Ri_\alpha - V_\alpha; \\ L\dfrac{\mathrm{d}i_\beta}{\mathrm{d}t} = e_\beta - Ri_\beta - V_\beta; \\ C\dfrac{\mathrm{d}V_{dc}}{\mathrm{d}t} = (S_\alpha i_\alpha + S_\beta i_\beta) - \dfrac{V_{dc}}{R_L}. \end{cases} \quad (3)$$

SMC-based DPC of three phase PWM rectifier. The block scheme of SMC-based DPC is given in Fig. 3. Sliding mode controllers are utilized to regulate the DC-link voltage, active power, and reactive power.

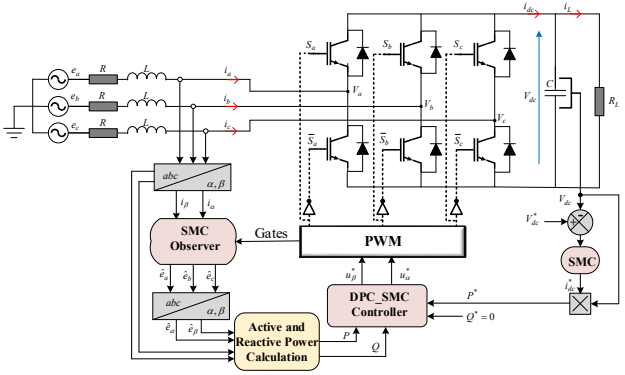

Fig. 3. DPC-SMC of three phase PWM rectifier

DC-link voltage sliding mode control. To determine the sliding surface, the general form is given as [10]:

$$S(t) = \left(\lambda + \frac{\mathrm{d}}{\mathrm{d}t}\right)^{n-1} e(t) + K\int_0^t e(t)\mathrm{d}t, \quad (4)$$

where $e(t)$ is the error between the reference and controlled values; λ, K are the strictly positive constants; n is the relative degree, which corresponds to the number of differentiations required for the output, until the control appears. In our case, n is set to 1, which gives the following sliding mode surface of DC-link voltage:

$$S_{dc}(t)=e_{dc}(t)+K_1\int e_{dc}(t)\mathrm{d}t\,, \tag{5}$$

where K_1 is the positive gain and:

$$e_{dc}(t)=V_{dc}^{*}(t)-V_{dc}(t), \tag{6}$$

by taking the first derivative of the sliding surface, we have:

$$\dot{S}_{dc}=\dot{e}_{dc}+K_1e_{dc}=\dot{V}_{dc}^{*}+\frac{V_{dc}}{R_LC}+K_1\left(V_{dc}^{*}-V_{dc}\right)-\frac{1}{C}i_{dc}\,. \tag{7}$$

In steady state, $\dot{S}_{dc}=S_{dc}=0$ which gives:

$$i_{dc}^{*}=C\dot{V}_{dc}^{*}+\frac{V_{dc}}{R_L}+K_1C\left(V_{dc}^{*}-V_{dc}\right)+K_{dc}\mathrm{sign}\left(S_{dc}\right), \tag{8}$$

where K_{dc} is the positive constant and the function sign(S_{dc}) is substituted by a smooth function (saturation), to minimize the chattering effect. It is given as:

$$\mathrm{sat}\left(S_{dc}\right)=\begin{cases}+1 & \text{if } S_{dc}>\gamma;\\ -1 & \text{if } S_{dc}<\gamma;\\ \dfrac{S_{dc}}{\gamma} & \text{if } \left|S_{dc}\right|\le\gamma,\end{cases} \tag{9}$$

where γ is the smooth factor.

Stability analysis. Let us take the Lyapunov's function as follows:

$$V_c=\frac{1}{2}S_{dc}^2\,. \tag{10}$$

The time derivative of this function is:

$$\dot{V}_c=S_{dc}\dot{S}_{dc}\,. \tag{11}$$

Substituting the derivative of the surface with its expression, we get:

$$\dot{V}_c=S_{dc}\begin{pmatrix}\dot{V}_{dc}^{*}-\left(\dot{V}_{dc}^{*}+\dfrac{V_{dc}}{R_LC}+K_1\left(V_{dc}^{*}-V_{dc}\right)\right)\\ -\dfrac{K_{dc}}{C}\mathrm{sign}\left(S_{dc}\right)+\dfrac{V_{dc}}{CR_L}+K_1\left(V_{dc}^{*}-V_{dc}\right)\end{pmatrix}, \tag{12}$$

$$\dot{V}_c=-S_{dc}\frac{K_{dc}}{C}\mathrm{sign}\left(S_{dc}\right)=-\frac{K_{dc}}{C}\left|S_{dc}\right|\,. \tag{13}$$

For $\dot{V}_c<0$, K_{dc} must be a positive constant. Finally the reference of active and reactive powers can be written as:

$$\begin{cases}P^{*}=V_{dc}i_{dc};\\ Q^{*}=0.\end{cases} \tag{14}$$

where i_{dc} is the DC-link current.

Active and reactive powers control. In this part, sliding mode controllers are introduced to ensure that the powers track their imposed desired values. The sliding surfaces of active and reactive powers are given as:

$$\begin{cases}S_P=e_P+K_2\int e_P\mathrm{d}t;\\ S_Q=e_Q+K_3\int e_Q\mathrm{d}t,\end{cases} \tag{15}$$

where:

$$\begin{cases}e_p=P-P^{*};\\ e_Q=Q-Q^{*},\end{cases} \tag{16}$$

where K_2 and K_3 are the positive gains. The surface derivatives are given as:

$$\begin{cases}\dot{S}_P=\dot{e}_P+K_2e_P;\\ \dot{S}_Q=\dot{e}_Q+K_3e_Q,\end{cases} \tag{17}$$

where:

$$\begin{cases}P=e_\alpha i_\alpha+e_\beta i_\beta;\\ Q=e_\beta i_\alpha-e_\alpha i_\beta.\end{cases} \tag{18}$$

Substituting active and reactive powers by their expressions and calculating the derivative of surface functions in matrix format, we can obtain:

$$\dot{S}_{PQ}=F+DU\,, \tag{19}$$

where:

$$D=\begin{bmatrix}-\dfrac{e_\alpha}{L} & -\dfrac{e_\beta}{L}\\ -\dfrac{e_\alpha}{L} & \dfrac{e_\beta}{L}\end{bmatrix},\quad U=\begin{bmatrix}V_\alpha\\ V_\beta\end{bmatrix}\text{ and}$$

$$F=\begin{bmatrix}\dot{V}_\alpha i_\alpha+\dot{V}_\beta i_\beta+\left(K_2-\dfrac{R}{L}\right)P+\dfrac{1}{L}\left(V_\alpha^2+V_\beta^2\right)-\dot{P}^{*}-K_2P^{*}\\ \dot{V}_\beta i_\alpha-\dot{V}_\alpha i_\beta+\left(K_3-\dfrac{R}{L}\right)Q-\dot{Q}^{*}-K_3Q^{*}\end{bmatrix},$$

where U is the vector control and F is theindependent term. In a steady state, to obtain the equivalent control term:

$$\dot{S}_{PQ}=0\,. \tag{20}$$

So:

$$U_{eq}=-D^{-1}F\,. \tag{21}$$

Finally, the control vector is given as:

$$U=U_{eq}+U_{NL}=-D^{-1}\left[F+K_{PQ}\mathrm{sign}\left(S_{PQ}\right)\right]. \tag{22}$$

The Lyapunov's function derivative is given by:

$$\begin{aligned}V_{PQ}&=S_{PQ}\dot{S}_{PQ}=\\ &=S_{PQ}\left(F+DU\right)=\\ &=S_{PQ}\left(F+D\left[-D^{-1}\left[F+K_{PQ}sign\left(S_{PQ}\right)\right]\right]\right)\end{aligned} \tag{23}$$

Simplification gives:

$$\dot{V}_{PQ}=-K_{PQ}\left|S_{PQ}\right|, \tag{24}$$

so $\dot{V}_{PQ}<0$ only if K_{PQ} is the positive constant.

SMC-based grid voltages observer. From the dynamical model of three phase boost rectifier in (α, β) frame , the current model can be given as:

$$\frac{\mathrm{d}i_g}{\mathrm{d}t}=\frac{1}{L}\left(e_g-Ri_g-V_g\right), \tag{25}$$

where $i_g=\left[i_\alpha\ i_\beta\right]^T$, $e_g=\left[e_\alpha\ e_\beta\right]^T$ and $V_g=\left[V_\alpha\ V_\beta\right]^T$.

The sliding mode observer model is expressed as:

$$\frac{\mathrm{d}\hat{i}_g}{\mathrm{d}t}=\frac{1}{L}\left(G\mathrm{sign}\left(S_g\right)-R\hat{i}_g-V_g\right), \tag{26}$$

where $S_g=i_g-\hat{i}_g$ is the observer's sliding surface of the

current, $\hat{i}_g = \begin{bmatrix}\hat{i}_\alpha & \hat{i}_\beta\end{bmatrix}^T$ is the estimated current vector, $G = \begin{bmatrix}G_1 & G_2\end{bmatrix}^T$ and G_1, G_2 are the positive gains.

From the previous equations (25), (26), we get:

$$\frac{\mathrm{d}S_g}{\mathrm{d}t} = \frac{1}{L}\left(e_g - RS_g - G\,\mathrm{sign}\left(S_g\right)\right), \tag{27}$$

when sliding mode is reached $\dot{S}_g = 0$, estimated grid voltages can be expressed as:

$$e_g = G\,\mathrm{sign}\left(S_g\right). \tag{28}$$

A low-pass filter (LPF) that also reduces the impact of the chattering phenomenon can be used to produce the grid voltages.

$$e_{gf} = LPF\left(G\,\mathrm{sign}\left(S_g\right)\right), \tag{29}$$

where $e_{gf} = \begin{bmatrix}e_{\alpha f} & e_{\beta f}\end{bmatrix}^T$ is the observer's filtered output in (α, β) frame.

The use of the LPF to minimize the chattering of a sliding mode observer has the disadvantage of attenuating the amplitude of the observed signal and creating a phase delay between the estimated and the signal to be estimated. To remedy this problem in [20] authors have proposed an adaptive algorithm to compensate the attenuation caused on the amplitude and the phase delay. This algorithm also has the advantage of being insensitive to the variation of the frequency of the grid voltage, which improves the precision of the observation illustrated in Fig. 4.

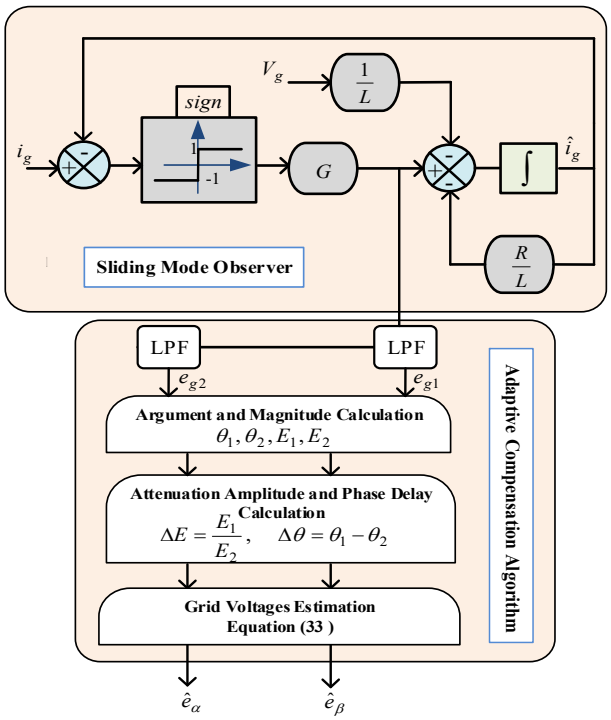

Fig. 4. Sliding mode-based grid voltages observer

The strategy of this algorithm is based on the use of two identical filters of low-pass type in a cascade (with same cut-off frequency ω_c).

$$\begin{cases} e_{g1} = \dfrac{\omega_c}{s+\omega_c} e_{gf}; \\ e_{g2} = \dfrac{\omega_c}{s+\omega_c} e_{g1}. \end{cases} \tag{30}$$

Amplitudes and arguments of outputs of previous filters can be calculated as follows:

$$\begin{cases} E_1 = \left\|e_{g1}\right\|; & \theta_1 = \arg\left(e_{g1}\right); \\ E_2 = \left\|e_{g2}\right\|; & \theta_2 = \arg\left(e_{g2}\right). \end{cases} \tag{31}$$

The errors in amplitudes and phases can be deduced as:

$$\begin{cases} \Delta E = \dfrac{E_1}{E_2}; \\ \Delta\theta = \theta_1 - \theta_2. \end{cases} \tag{32}$$

Finally, we can get the expressions of the estimated grid voltages by taking into account the compensation of the amplitude attenuation and the phase deviation, as:

$$\begin{cases} \hat{e}_\alpha = E_2 \Delta E^2 \cos\left(\theta_2 + 2\Delta\theta\right); \\ \hat{e}_\beta = E_2 \Delta E^2 \sin\left(\theta_2 + 2\Delta\theta\right). \end{cases} \tag{33}$$

Load resistance observer [21]. From the DC side voltage equation, the following two equations can be written as:

$$\begin{cases} \dfrac{\mathrm{d}V_{dc}}{\mathrm{d}t} = \dfrac{1}{C}\left(S_\alpha i_\alpha + S_\beta i_\beta\right) - \dfrac{V_{dc}}{CR_L}; \\ \dfrac{\mathrm{d}\hat{V}_{dc}}{\mathrm{d}t} = \dfrac{1}{C}\left(S_\alpha i_\alpha + S_\beta i_\beta\right) - \dfrac{\hat{V}_{dc}}{CR_{L0}} + \lambda\,\mathrm{sign}\left(e_V\right), \end{cases} \tag{34}$$

where $\hat{V}_{dc}$ is the observed DC-link voltage and R_{L0} is the nominal value of load resistance, the error observation is given as:

$$e_V = V_{dc} - \hat{V}_{dc}. \tag{35}$$

In addition, the error dynamic equation:

$$\begin{aligned} \frac{\mathrm{d}e_V}{\mathrm{d}t} &= \frac{\mathrm{d}V_{dc}}{\mathrm{d}t} - \frac{\mathrm{d}\hat{V}_{dc}}{\mathrm{d}t} = \\ &= -\left(\frac{V_{dc}}{CR_L} - \frac{\hat{V}_{dc}}{CR_{L0}}\right) - \lambda\,\mathrm{sign}\left(e_V\right), \end{aligned} \tag{36}$$

where λ is the positive constant that satisfies:

$$\lambda > \left| -\left(\frac{V_{dc}}{CR_L} - \frac{\hat{V}_{dc}}{CR_{L0}}\right)\right|, \tag{37}$$

when sliding mode is reached in finite time, equivalent control:

$$V_{dc} = \hat{V}_{dc} \Rightarrow \left(\frac{\hat{V}_{dc}}{CR_L} - \frac{V_{dc}}{CR_{L0}}\right) = V_{R,eq}, \tag{38}$$

where $V_{R,eq}$ is the equivalent control [22, 23] of the observer. Its estimate $\hat{V}_{R,eq}$ can be generated by the LPF:

$$\hat{V}_{R,eq} = LPF\left(\lambda\,\mathrm{sign}\left(e_V\right)\right). \tag{39}$$

Finally, the estimated load resistance can be deduced from its nominal value and the observer's output:

$$\hat{R}_L = -\frac{C\hat{V}_{R,eq}}{\hat{V}_{dc}} + R_{L0}. \tag{40}$$

Simulation results and discussions. To illustrate the effectiveness and the feasibility of the enhanced DPC based on sliding mode approach for control and observation, simulation studies were carried out with MATLAB/Simulink under several operations conditions. For this purpose, all three-phase PWM rectifier parameters are summarized in Table 1.

Table 1

Three phase PWM rectifier parameters

Parameters	Values
Grid frequency f, Hz	50
Grid voltage V, V	120
Reference of DC-link voltage V_{dc}^{*}, V	300
Grid side inductance L, mH	16
Grid side resistance R, Ω	0.1
DC-link capacitor C, μF	1100
Load resistance R_L, Ω	40→80
PWM frequency f_P, kHz	15

Several tests were carried out using MATLAB/Simulink to test the performance of DPC control based on SMC. In the first test, and for a variable load profile depicted by Fig. 5 the DPC-SMC block diagram is simulated for two operating conditions: with grid voltage measurement from 0 to 1.5 s and then without grid voltage sensor using a sliding mode observer from 1.5 s to 3 s.

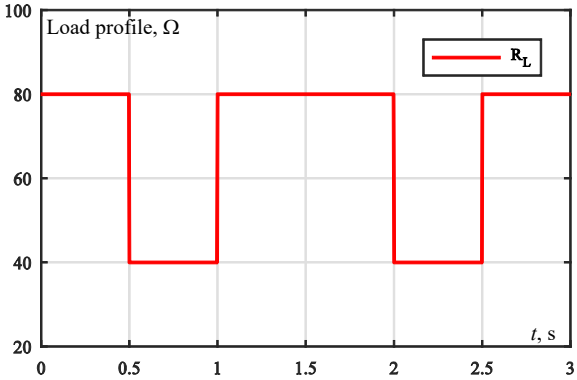

Fig. 5. Load profile

The curves obtained are illustrated by Fig. 6–11 and the following comments can be carried out.

In the presence of disturbance and according to Fig. 6, the DC-link voltage tracks perfectly its imposed reference (300 V) with a disturbance rejection considered good at the moments of load variation.

Figure 7 shows the evolution of active and reactive power. It is very clear that the active power has behavior identical to that of the reference generated reflecting the applied load. It is equal to 1195 W for R = 80 Ω and then increases to 2300 W when the load passes to R = 40 Ω. On the same Fig. 7, it can be seen that reactive power has a zero average value, which guarantees a unitary power factor, and therefore the grid current and voltage are always in phase (Fig. 9).

Under a variable load profile, Fig. 10 shows the waveforms of the three voltages measured and estimated using a sliding mode-based observer. Whatever the operating conditions, the introduction of the voltage observer at time 1.5 s gives good results and the estimated grid voltages show no amplitude attenuation or phase delay compared to the actual signal. This is justified by the introduction of a compensation algorithm.

As for the power quality, for both with and without grid voltage observer operating conditions, the THD is less than 5 %, which is in accordance with IEEE 519 International Standards Fig. 11 for various operating conditions.

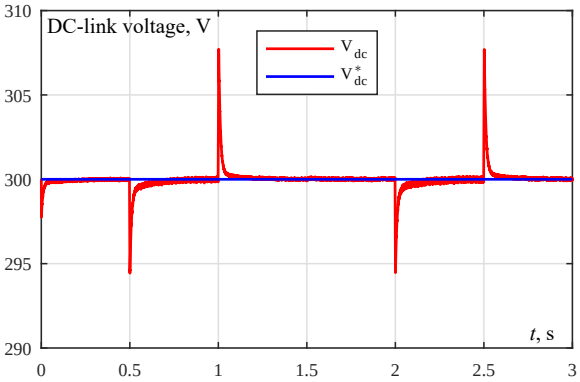

Fig. 6. DC-link voltage regulation

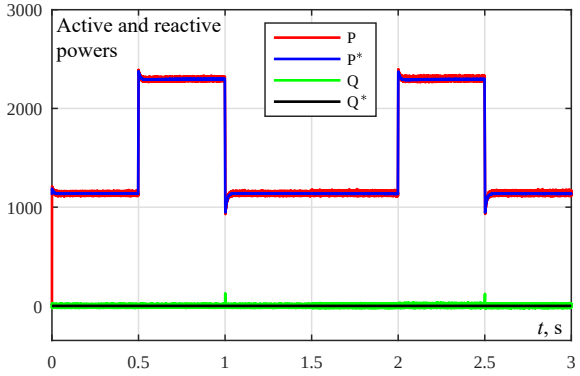

Fig. 7. Active and reactive powers

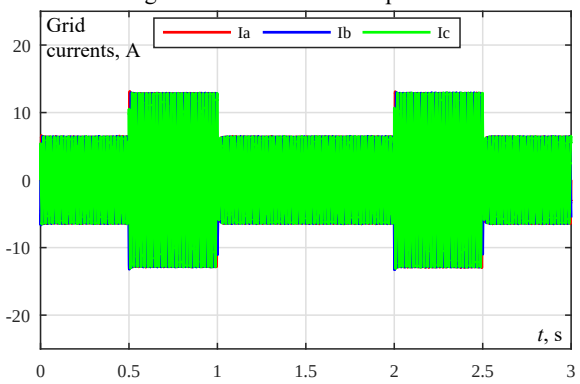

Fig. 8. Three-phase grid currents

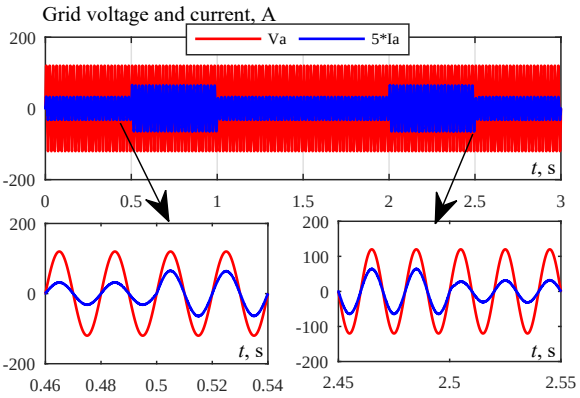

Fig. 9. Grid voltage and current

Another test is done in open loop to illustrate the advantages of the observer associated with double LPFs and a compensation algorithm. Examination of Fig. 12, 13 shows that the errors in amplitude and phase are very noticeable when the observer uses a single LPF. At time t = 0.5 s, the system based on double LPFs and a compensation algorithm is introduced. It is easy to notice that the amplitude attenuation and the phase delay can be compensated.

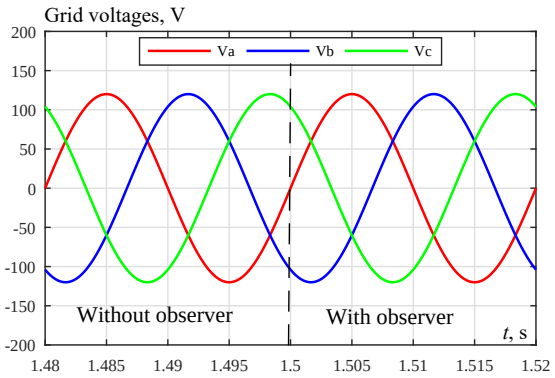

Fig. 10. Grid voltage with and without observer

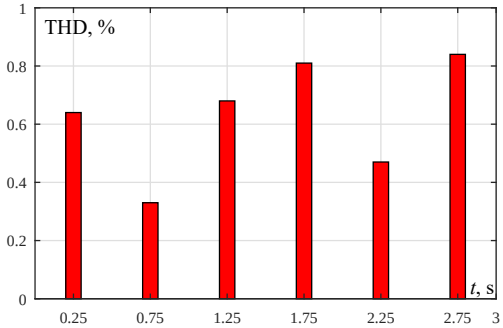

Fig. 11. THD of grid current

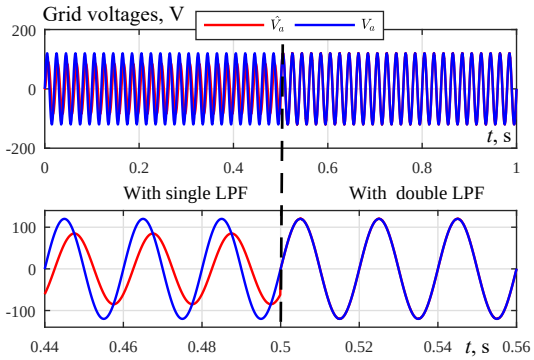

Fig. 12. Observed grid line voltage with compensation algorithm

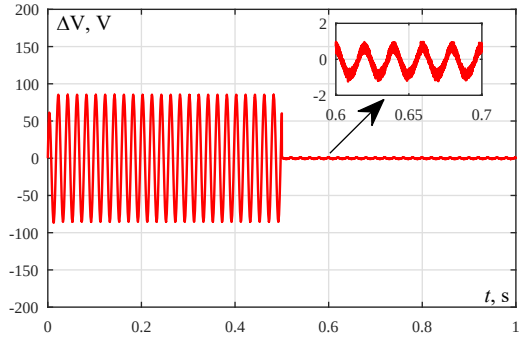

Fig. 13. Grid voltage observation error

The second test evaluates the DPC-SMC without a grid voltage sensor and with online estimation of the load variation using a sliding mode observer and under a load variable profile.

The results show that the performance of the sensorless DPC-SMC control is always better. Figure 14 shows that the observer accurately estimates the load variation which is reflected by the low estimation errors shown in Fig. 15.

In Fig. 16, the measured the DC-link voltage tracks perfectly its reference, which confirms the good design of the voltage controller.

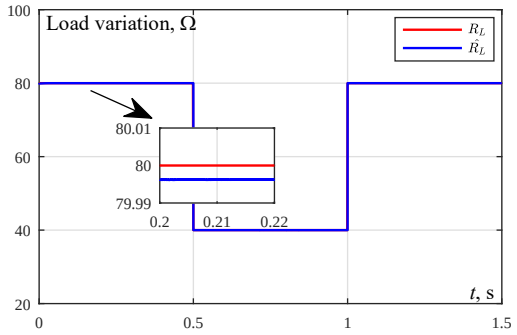

Fig. 14. Load observation

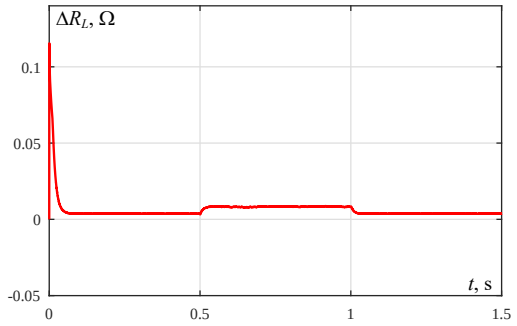

Fig. 15. Error in load estimation

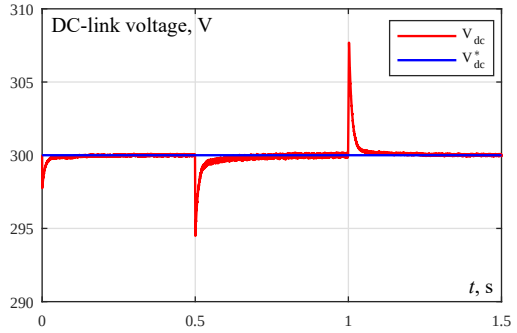

Fig. 16. Behavior of DC-link voltage

For Fig. 17 depicting the evolution of the instantaneous active and reactive powers, it is very clear that they present a fast dynamic and track their references without overshoot.

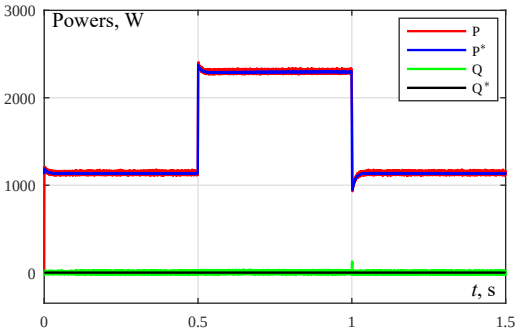

Fig. 17. Instantaneous active and reactive power

The high quality of the grid line current (sinusoidal waveform) is confirmed by a good unit power factor, as shown in Fig. 19, and by the low THD values indicated by the bars in Fig. 18 for various operating conditions.

Table 2 presents a comparison between DPC-SMC and other control techniques based on several terms.

Table 2

Comparison between conventional control strategies and DPC-SMC

	DPC-SMC	DPC [24]	Other techniques [25]
THD, %	1.13	3.17	3.35→12.2
Power factor	1	1	0.98→0.99

From this comparative table, the DPC-SMC control shows its superiority over the other techniques.

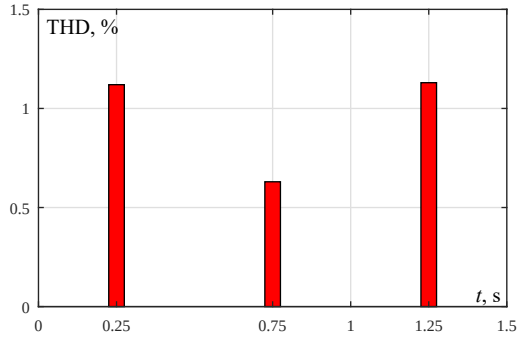

Fig. 18. THD of grid current

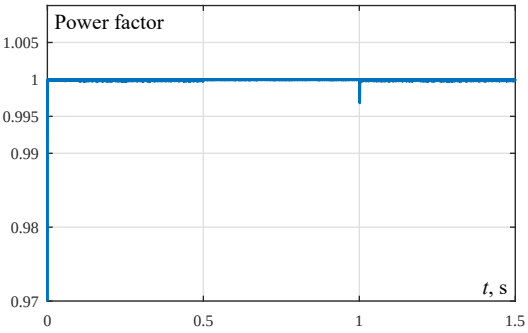

Fig. 19. Power factor

Conclusions.

In this paper, the classical direct power control has been combined with a sliding mode control to control active and reactive power and to ensure an accurate regulation of DC-link voltage. To eliminate the need for voltage sensors and to get the online variation of load resistance, sliding mode based observers have been designed for this purpose. Through a series of tests, especially in the presence of disturbances, it has been shown that:

1. The sliding mode offers a clear improvement to the DC-link voltage regulation regardless of the load profile.

2. The combination of the sliding mode approach with direct power control has eliminated the need for a switching table, thus reducing the control complexity.

3. High performance instantaneously decoupled power control achieved using a sliding mode control which provides a unity power factor.

4. The sliding mode-based grid voltage observer combined with the compensation algorithm provided accurate results with minimum chattering compared to the single low-pass filter case.

5. A good power quality is justified by a lower total harmonic distortion value.

6. The direct power control – sliding mode control gives better performance than conventional techniques with a total harmonic distortion value less than 5 % and a power factor close to unity.

Conflict of interest. The authors declare that they have no conflicts of interest.

REFERENCES

1. Bouafia A. *Techniques de commande prédictive et floue pour les systèmes électroniques de puissance : application aux redresseurs MLI*. Doctoral Thesis, University of Setif, Algeria, 2010. (Fra).

2. Bechouche A., Seddiki H., Abdeslam D.O., Rahoui A., Triki Y., Wira P. Predictive direct power control with virtual-flux estimation of three-phase PWM rectifiers under nonideal grid voltages. *2018 IEEE International Conference on Industrial Technology (ICIT)*, 2018, pp. 806-811. doi: https://doi.org/10.1109/ICIT.2018.8352281.

3. Bechouche A., Seddiki H., Abdeslam D.O., Mesbah K. Adaptive AC filter parameters identification for voltage-oriented control of three-phase voltage-source rectifiers. *International Journal of Modelling, Identification and Control*, 2015, vol. 24, no. 4, pp. 319-331. doi: https://doi.org/10.1504/IJMIC.2015.072985.

4. Bouafia A., Gaubert J.-P., Krim F. Predictive Direct Power Control of Three-Phase Pulsewidth Modulation (PWM) Rectifier Using Space-Vector Modulation (SVM). *IEEE Transactions on Power Electronics*, 2010, vol. 25, no. 1, pp. 228-236. doi: https://doi.org/10.1109/TPEL.2009.2028731.

5. Norniella J.G., Cano J.M., Orcajo G.A., Rojas C.H., Pedrayes J.F., Cabanas M.F., Melero M.G. Improving the Dynamics of Virtual-Flux-Based Control of Three-Phase Active Rectifiers. *IEEE Transactions on Industrial Electronics*, 2014, vol. 61, no. 1, pp. 177-187. doi: https://doi.org/10.1109/TIE.2013.2245614.

6. Rahoui A., Bechouche A., Seddiki H., Abdeslam D.O. Grid Voltages Estimation for Three-Phase PWM Rectifiers Control Without AC Voltage Sensors. *IEEE Transactions on Power Electronics*, 2018, vol. 33, no. 1, pp. 859-875. doi: https://doi.org/10.1109/TPEL.2017.2669146.

7. Friedli T., Hartmann M., Kolar J.W. The Essence of Three-Phase PFC Rectifier Systems – Part II. *IEEE Transactions on Power Electronics*, 2014, vol. 29, no. 2, pp. 543-560. doi: https://doi.org/10.1109/TPEL.2013.2258472.

8. Zhang Z., Xie Y., Le J., Chen L. Decoupled State-Feedback and Sliding-Mode Control for Three-Phase PWM Rectifier. *2009 Asia-Pacific Power and Energy Engineering Conference*, 2009, pp. 1-5. doi: https://doi.org/10.1109/APPEEC.2009.4918252.

9. Noguchi T., Tomiki H., Kondo S., Takahashi I. Direct power control of PWM converter without power-source voltage sensors. *IEEE Transactions on Industry Applications*, 1998, vol. 34, no. 3, pp. 473-479. doi: https://doi.org/10.1109/28.673716.

10. Barkat S., Tlemcani A., Nouri H. Direct power control of the PWM rectifier using sliding mode control. *International Journal of Power and Energy Conversion*, 2011, vol. 2, no. 4, pp. 289-306. doi: https://doi.org/10.1504/IJPEC.2011.041883.

11. Escobar G., Stankovic A.M., Carrasco J.M., Galvan E., Ortega R. Analysis and design of direct power control (DPC) for a three phase synchronous rectifier via output regulation subspaces. *IEEE Transactions on Power Electronics*, 2003, vol. 18, no. 3, pp. 823-830. doi: https://doi.org/10.1109/TPEL.2003.810862.

12. Vazquez S., Sanchez J.A., Carrasco J.M., Leon J.I., Galvan E. A Model-Based Direct Power Control for Three-Phase Power Converters. *IEEE Transactions on Industrial Electronics*, 2008, vol. 55, no. 4, pp. 1647-1657. doi: https://doi.org/10.1109/TIE.2008.917113.

13. Malinowski M., Kazmierkowski M.P., Hansen S., Blaabjerg F., Marques G.D. Virtual-flux-based direct power control of three-phase PWM rectifiers. *IEEE Transactions on Industry Applications*, 2001, vol. 37, no. 4, pp. 1019-1027. doi: https://doi.org/10.1109/28.936392.

14. Malinowski M., Jasinski M., Kazmierkowski M.P. Simple Direct Power Control of Three-Phase PWM Rectifier Using Space-Vector Modulation (DPC-SVM). *IEEE Transactions on Industrial Electronics*, 2004, vol. 51, no. 2, pp. 447-454. doi: https://doi.org/10.1109/TIE.2004.825278.

15. Cichowlas M., Malinowski M., Kazmierkowski M.P., Sobczuk D.L., Rodriguez P., Pou J. Active Filtering Function of Three-Phase PWM Boost Rectifier Under Different Line Voltage Conditions. *IEEE Transactions on Industrial Electronics*, 2005, vol. 52, no. 2, pp. 410-419. doi: https://doi.org/10.1109/TIE.2005.843915.

16. Antoniewicz P., Kazmierkowski M.P. Virtual-Flux-Based Predictive Direct Power Control of AC/DC Converters With Online Inductance Estimation. *IEEE Transactions on Industrial*

Electronics, 2008, vol. 55, no. 12, pp. 4381-4390. doi: https://doi.org/10.1109/TIE.2008.2007519.
17. Francis M. *Performance of Direct Power Controlled Grid-connected Voltage Source Converters*. Doctoral Thesis, University of Newcastle, England, 2017.
18. Bouraghda S., Sebaa K., Bechouat M., Sedraoui M. An improved sliding mode control for reduction of harmonic currents in grid system connected with a wind turbine equipped by a doubly-fed induction generator. *Electrical Engineering & Electromechanics*, 2022, no. 2, pp. 47-55. doi: https://doi.org/10.20998/2074-272X.2022.2.08.
19. Guezi A., Bendaikha A., Dendouga A. Direct torque control based on second order sliding mode controller for three-level inverter-fed permanent magnet synchronous motor: comparative study. *Electrical Engineering & Electromechanics*, 2022, no. 5, pp. 10-13. doi: https://doi.org/10.20998/2074-272X.2022.5.02.
20. Guo L., Li Y., Jin N., Dou Z., Wu J. Sliding mode observer-based AC voltage sensorless model predictive control for grid-connected inverters. *IET Power Electronics*, 2020, vol. 13, no. 10, pp. 2077-2085. doi: https://doi.org/10.1049/iet-pel.2019.1075.
21. Shtessel Y., Baev S., Biglari H. Unity Power Factor Control in Three-Phase AC/DC Boost Converter Using Sliding Modes. *IEEE Transactions on Industrial Electronics*, 2008, vol. 55, no. 11, pp. 3874-3882. doi: https://doi.org/10.1109/TIE.2008.2003203.
22. Edwards C., Spurgeon S. *Sliding Mode Control*. CRC Press, 1998. doi: https://doi.org/10.1201/9781498701822.
23. Utkin V., Gulder J., Shijun M. *Sliding Mode Control in Electromechanical Systems. 2nd ed.* New York, Taylor & Francis, 1999.
24. Lamterkati J., Khafallah M., Ouboubker L. A New DPC for Three-phase PWM rectifier with unity power factor operation. *International Journal of Advanced Research in Electrical, Electronics and Instrumentation Engineering*, 2014, vol. 3, no. 4, pp. 8273-8285.
25. Darshanam M.D., Hariharan D.R. Research on Three phase Voltage Source PWM Rectifier Based on Direct Current Control. *International Journal of Engineering and Advanced Technology*, 2019, vol. 9, no. 1, pp. 6864-6867. doi: https://doi.org/10.35940/ijeat.A2989.109119.

Received 11.09.2022
Accepted 21.12.2022
Published 07.03.2023

Djamel Sakri [1], *Doctor of Electrotechnical, Professor,*
Hichem Laib [1], *Doctor of Electrotechnical, Professor,*
Salah Eddine Farhi [1], *Doctor of Electrotechnical,*
Noureddine Golea [1], *Doctor of Electrotechnical, Professor,*
[1] Laboratory of Electrical Engineering and Automatic (LGEA), Larbi Ben M'hidi University Oum El Bouaghi, 04000, Algeria,
e-mail: sk_djamel@yahoo.fr (Corresponding author),
hichem_elt@yahoo.fr, salahfarhi04@gmail.com,
nour_golea@yahoo.fr

How to cite this article:
Sakri D., Laib H., Farhi S.E., Golea N. Sliding mode approach for control and observation of a three phase AC-DC pulse-width modulation rectifier. *Electrical Engineering & Electromechanics*, 2023, no. 2, pp. 49-56. doi: https://doi.org/10.20998/2074-272X.2023.2.08